Protein Science (1993), *2*, 1966–1974. Cambridge University Press. Printed in the USA.

Amide proton exchange rates of oxidized and reduced *Saccharomyces cerevisiae* iso-1-cytochrome *c*

JENNIFER L. MARMORINO,[1] DOUGLAS S. AULD,[1,3] STEPHEN F. BETZ,[1,4] DONALD F. DOYLE,[1] GREGORY B. YOUNG,[2] AND GARY J. PIELAK[1]

[1] Department of Chemistry and [2] Department of Biochemistry and Biophysics, University of North Carolina, Chapel Hill, North Carolina 27599

(RECEIVED June 4, 1993; ACCEPTED August 17, 1993)

Abstract

Proton NMR spectroscopy was used to determine the rate constant, k_{obs}, for exchange of labile protons in both oxidized (Fe(III)) and reduced (Fe(II)) iso-1-cytochrome *c*. We find that slowly exchanging backbone amide protons tend to lack solvent-accessible surface area, possess backbone hydrogen bonds, and are present in regions of regular secondary structure as well as in Ω-loops. Furthermore, there is no correlation between k_{obs} and the distance from a backbone amide nitrogen to the nearest solvent-accessible atom. These observations are consistent with the local unfolding model. Comparisons of the free energy change for denaturation, ΔG_d, at 298 K to the free energy change for local unfolding, ΔG_{op}, at 298 K for the oxidized protein suggest that certain conformations possessing higher free energy than the denatured state are detected at equilibrium. Reduction of the protein results in a general increase in ΔG_{op}. Comparisons of ΔG_d to ΔG_{op} for the reduced protein show that the most open states of the reduced protein possess more structure than its chemically denatured form. This persistent structure in high-energy conformations of the reduced form appears to involve the axially coordinated heme.

Keywords: amide proton exchange; cytochrome *c*; denaturation; NMR; protein stability

Many small globular proteins denature via a two-state mechanism. That is, at equilibrium they exist primarily in either the native state or the denatured state. Most techniques for assessing denaturation, such as circular dichroism, fluorescence, and calorimetry, measure global features and are therefore insensitive to small populations of conformations that may coexist within the native state. In contrast, proton NMR spectroscopy is a technique that monitors specific, local interactions and can supply evidence for poorly populated conformations that exist at equilibrium (Englander & Kallenbach, 1984). In this paper, *Saccharomyces cerevisiae* iso-1-cytochrome *c* is used as a model for studying protein backbone amide proton exchange in general.

Cytochromes *c* are small globular proteins that effect the penultimate interprotein electron transfer reaction of the eukaryotic respiratory chain by shuttling between the reduced, diamagnetic (Fe(II), d^6) and the oxidized, paramagnetic (Fe(III), low spin d^5) states. Cytochromes *c* are good models for studying globular proteins because over 100 sequences are known, they exhibit reversible two-state denaturation, several high-resolution crystal structures are available, they yield high-quality NMR data, protein variants are produced readily, and there are simple biological screens for function.

Our version of wild-type yeast iso-1-cytochrome *c*, the C102T variant (Cutler et al., 1987), is identical structurally to the wild-type protein (Gao et al., 1990, 1991; Berghuis & Brayer, 1992) but is more amenable to biophysical studies (Betz & Pielak, 1992). Compared to higher eukaryotic cytochromes *c*, those from plants and fungi possess N-terminal extensions (Moore & Pettigrew, 1990). The five residues of the extension in iso-1-cytochrome *c* are labeled −5 to −1 to facilitate comparisons with cytochromes *c* from higher eukaryotes.

We used NMR to measure k_{obs} for individual backbone amide protons in both oxidation states of the C102T variant. Rate constants are compared to properties of the exchangeable sites. These properties include solvent accessibility, distance to the surface of the protein, hydro-

Reprint requests to: Gary J. Pielak, Department of Chemistry, University of North Carolina, Chapel Hill, North Carolina 27599.

[3] Present address: Department of Biology, Massachusetts Institute of Technology, Cambridge, Massachusetts 02138.

[4] Present address: Dupont-Merck Pharmaceutical Company, P.O. Box 80328, Wilmington, Delaware 19880-0328.

gen bonding, and secondary structure. The implications of these comparisons with respect to models for amide proton exchange are discussed.

When a protein in H_2O is transferred to D_2O, the exchange of amide and other labile protons for deuterons can be described by Equation 1 (Linderstrøm-Lang, 1958):

$$N(H) \underset{k_2}{\overset{k_1}{\rightleftharpoons}} N'(H) \xrightarrow{k_3} N'(D) \underset{k_2}{\overset{k_1}{\rightleftharpoons}} N(D). \quad (1)$$

The equilibrium constant, K, for the first step is k_1/k_2. The labile sites possessing a proton or a deuteron, respectively, are $N(H)$ and $N(D)$. As discussed below, the presumed nature of N' depends on the model used to interpret the data. The term k_3 is the rate constant for exchange once the labile site contacts the catalyst. This second step is primarily base catalyzed above pH 4 (McDonald & Phillips, 1973; Patel & Canuel, 1976; Englander & Kallenbach, 1984), but water itself can also react directly (Gregory et al., 1983). Acid catalysis occurs at lower pH (Perrin, 1989). The second step is essentially irreversible because the concentration of the D_2O is five orders of magnitude greater than the protein.

If $k_2 \gg k_1$, the rate constant describing the disappearance of $N(H)$, k_{obs}, equals $k_1k_3/(k_2 + k_3)$. Hvidt and Nielsen (1966) described two limiting cases depending on the relative values of k_2 and k_3. If $k_3 \gg k_2$, k_{obs} equals k_1. This is the EX_1 limit. If $k_3 \ll k_2$, k_{obs} equals k_1k_3/k_2, which reduces to Kk_3. This is the EX_2 limit.

There are two main models for labile proton exchange. In the solvent penetration model (Ellis et al., 1975; Woodward & Hilton, 1979), K is the product of an equilibrium constant for creating a channel in the protein and a distribution coefficient for the catalyst between bulk solution and the point in the channel where exchange occurs. The term k_3 is the rate constant for exchange once the labile proton and catalyst meet inside the protein. For the penetration model, exchange rate is expected to be a function of the distance from the channel and need not depend on secondary or tertiary structure. Another prediction of the penetration model is that vastly different rates may be observed for residues close in the primary structure because one residue may be part of one channel, whereas its neighbor may be part of another. Solvent penetration has been invoked as a possible explanation for very slowly exchanging backbone amide protons of lysozyme (Pedersen et al., 1993).

In the local unfolding model, K is written K_{op} and describes any opening of the peptide chain that exposes a labile site to the catalyst. The term k_3 is the rate constant for exchange of the exposed proton. For this model, k_3 is usually determined from exchange data for peptides and modified by factors that depend on sequence, temperature, and pH (Molday et al., 1972; Englander et al., 1979; Bai et al., 1993; Connelly et al., 1993). Local unfolding is expected to be correlated with hydrogen bonding and the presence of secondary structure. For the local unfolding model in the EX_2 limit, K_{op} is calculated by dividing k_{obs} by k_3. The concomitant free energy change for local unfolding, ΔG_{op}, is $-RT\ln(K_{op})$. The two models are equivalent when channels become large enough to expose labile protons to bulk solvent or when motions of local unfolding units become small enough to at least partially exclude the catalyst.

How can the EX_1 and EX_2 limits be distinguished? Assuming that k_1 and k_2 are pH independent, for the EX_2 limit, k_{obs} should increase with pH because exchange from $N'(H)$ is base catalyzed and k_3 is rate limiting. The pH dependence is model independent except that the models predict different minima for k_{obs} as a function of pH (Englander & Kallenbach, 1984). Pedersen et al. (1993) studied the pH dependence of k_{obs} for lysozyme and concluded that data for all but the most buried and most slowly exchanging backbone amide protons are consistent with the EX_2 limit. For local unfolding in the EX_1 limit, every unfolding event results in exchange; sites within the same unfolding unit are expected to exchange together. Roder et al. (1985) called this "correlated exchange" and presented data for bovine pancreatic trypsin inhibitor that suggest the EX_1 limit will occur for stable proteins in basic solutions—conditions that tend to maximize k_3 and minimize k_2. Using mass spectroscopic techniques, Zhang and Smith (1993) showed that at pH 7 near room temperature, backbone amide proton exchange in horse cytochrome *c* is not correlated, and thus is consistent with the EX_2 limit.

Results

Determination of k_{obs}

Of the 103 residues that possess backbone amide protons, 36 in the oxidized protein and 47 in the reduced protein exchange slowly enough under the conditions used (pH 4.6, 298 K) to be observed in at least the first two spectra. Twenty-five of these amide protons are common to both oxidation states.

Plots of proton occupancy versus time are shown in Figure 1. Values of k_{obs} were calculated using a nonlinear least-squares fitting procedure and were found to range between approx. 0.1 and 10^{-3} h^{-1}. For the oxidized protein, Leu 98 possesses a slowly exchanging amide proton with a k_{obs} (±SD) of 1.0 (±0.4) × 10^{-3} h^{-1}, Phe 36 possesses a rapidly exchanging amide proton with a k_{obs} of 0.11 (±0.01) h^{-1}, and Lys 11 possesses a moderately exchanging amide proton with a k_{obs} of 1.6 (±0.2) × 10^{-2} h^{-1}. The range is similar for the reduced protein, with Ile 75 (k_{obs} = 8 [±1] × 10^{-4} h^{-1}), Lys 54 (k_{obs} = 7.1 [±0.4] × 10^{-2} h^{-1}), and Arg 13 (k_{obs} = 3.2 [±0.4] × 10^{-2} h^{-1}) exhibiting typical slow, fast, and moderate exchange.

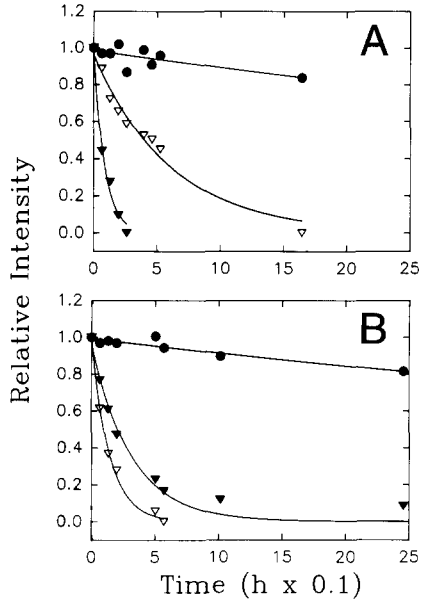

Fig. 1. Plots of relative intensity versus time for the amide-alpha crosspeaks of Leu 98 (●), Lys 11 (▽), and Phe 36 (▼) in the oxidized protein (**A**) and Ile 75 (●), Lys 54 (▽), and Arg 13 (▼) in the reduced protein (**B**). Curves represent nonlinear least squares fits of the data to a first-order process.

There are several explanations for the lack of information from certain residues. Of the 108 residues of the C102T variant, four (at positions 25, 30, 71, and 76) are prolines. Unlike many other eukaryotic cytochromes *c*, the N-terminal residue of iso-1-cytochrome *c* is not acetylated and the protons of the free amine remain unassigned. Both Lys 4 and Cys 14 remain unassigned in the oxidized protein; Thr −5, Glu −4, Gly 83, and Gly 84 are unassigned in both oxidation states. For certain residues, backbone amide protons exchange so slowly that occupancy does not change significantly over the course of the experiment. The amide protons of residues Lys 87 and Tyr 97 in the oxidized protein and Phe 10, Leu 15, His 18, Trp 59, Thr 69, and Leu 98 in the reduced protein belong to this group. An upper limit for k_{obs} of 1.8×10^{-3} h^{-1} was estimated for the amide protons of Lys 87 and Tyr 97. Upper limits of 7.8×10^{-4} h^{-1} and 1.2×10^{-3} h^{-1} were estimated for Phe 10 and Leu 15, respectively. For the remainder of the residues in the list, k_{obs} is assumed to be even smaller, and an apparent value of 1.6×10^{-4} h^{-1} is assigned. Data for Phe 10 in the oxidized protein and for Ser 40 in the reduced protein show non-monoexponential behavior. Certain backbone amide protons exhibit anomalous fluctuations in occupancy. This group includes Tyr 46 and Leu 94 in the reduced protein and Met 64 in both oxidation states. Certain backbone amide protons exchange so quickly that crosspeaks are visible only in the first spectrum. This group includes Leu 9, Cys 17, His 26, Ile 53, Val 57, Asn 70, Phe 82, and Asp 90 in the oxidized protein, and Lys 5, Lys 11, and Leu 85 in the reduced protein. For other residues, amide-alpha crosspeaks were not observed at the first time point.

In addition to backbone amide protons, two other labile sites were studied in the reduced state. These were the π proton of the axial histidine heme ligand, His 18 ($k_{obs} = 1.2$ [±0.5] $\times 10^{-2}$ h^{-1}), and the indole proton of Trp 59 ($k_{obs} = 8$ [±3] $\times 10^{-2}$ h^{-1}). In the oxidized state these protons exchange completely before the first time point.

Determination of K_{op}

For each residue k_{obs} was divided by k_3 to give K_{op}. The value of k_3 for each site was calculated as described by Bai et al. (1993) and Connelly et al. (1993). The protection factor, P, is K_{op}^{-1}. Log P is proportional to ΔG_{op} ($\Delta G_{op} = 2.3RT \log P$). Histograms of log P versus residue number for the oxidized and reduced proteins are presented in Figures 2 and 3, respectively. Filled bars are used for residues where only upper or lower limits are assigned. For very quickly exchanging backbone amide protons, the filled bar is set to 1.5. For very slowly exchanging backbone amide protons the bar is set at 5.5.

A histogram of $\log P_{\text{oxidized}} - \log P_{\text{reduced}}$ versus residue number is presented in Figure 4. Open bars are used for residues where k_{obs} can be calculated in both oxidation states. Filled bars are used for residues where it is only possible to determine the sign of $\log P_{\text{oxidized}} - \log P_{\text{reduced}}$ because one of the k_{obs} values is an estimate.

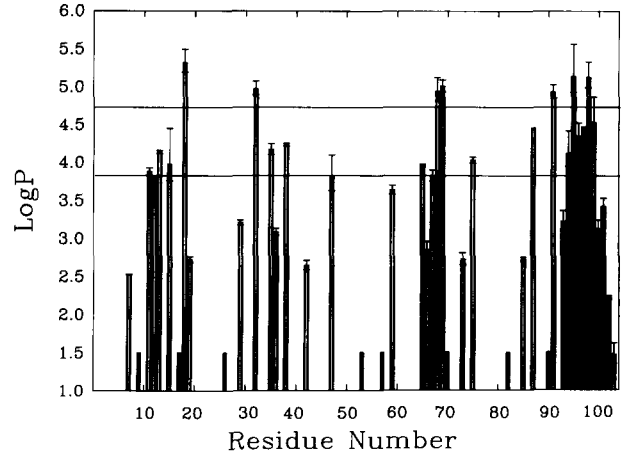

Fig. 2. Histogram of residue number versus the logarithm of the protection factor, log P, for the oxidized protein. Error bars were calculated from the standard deviation of k_{obs}. Error bars are not shown for Lys 87 and Tyr 97 because only upper limits are available (see Results). Solid bars to 1.5 represent amide protons whose amide-alpha crosspeaks were observed only in the first spectrum. Horizontal lines represent log P values equivalent to the lower and upper limits of ΔG_d at 298 K (see Results).

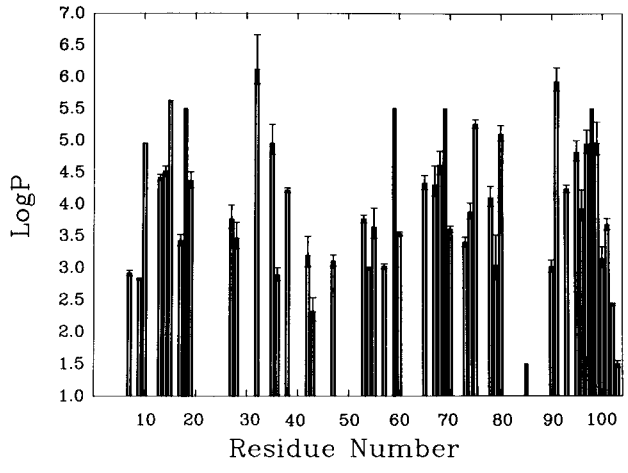

Fig. 3. Histogram of residue number versus the logarithm of the protection factor, log P, for the reduced protein. Error bars were calculated from the standard deviation of k_{obs}. Error bars are not shown for Phe 10 and Leu 15 because only upper limits are available (see Results). Solid bars to 1.5 represent amide protons whose amide-alpha crosspeaks were observed only in the first spectrum. Solid bars to 5.5 represent amide protons that exchange too slowly to allow calculation of k_{obs}.

Backbone amide protons with large protection factors

At pH 4.6 and 298 K in H_2O, ΔG_d for the oxidized protein ranges from 5.2 to 6.5 kcal mol^{-1}, depending on the probe used to monitor denaturation (Betz & Pielak, 1992; D. Cohen & G. Pielak, unpubl.). Horizontal lines corresponding to these values are drawn in Figure 2. We also examined the absorbance-detected thermal denaturation of the C102T variant in D_2O and found that ΔG_d at pH 4.6 and 298 K is approx. 5.8 kcal mol^{-1} (D. Michael & G. Pielak, unpubl.). Values of ΔG_{op} for His 18, Leu 32, Leu 68, Thr 69, Arg 91, Ile 95, and Leu 98 are greater than the upper limit for ΔG_d. The observation of states with higher free energy than the denatured state was unexpected, so we questioned our values of k_{obs} and the calculated values of k_3. All time points for the listed residues were used to determine k_{obs}, so there is no bias from omitting points from the fit. Next, the validity of k_3 values was considered because error bars in Figures 2–4 reflect uncertainty in k_{obs} only. To bring ΔG_{op} values of the seven residues within the range for ΔG_d, k_3 would have to decrease by a factor between 2 and 4 (depending on the residue) for the upper limit and between 14 and 33 for the lower limit of ΔG_d. We noted that none of the residue types in the list above is unique and that k_3 values for these residue types at other positions yield ΔG_{op} values consistent with ΔG_d. We also noted that several of the residues are close in primary structure. Therefore, the largest values of ΔG_{op} are not due to poor protein data or systematically low values of k_3.

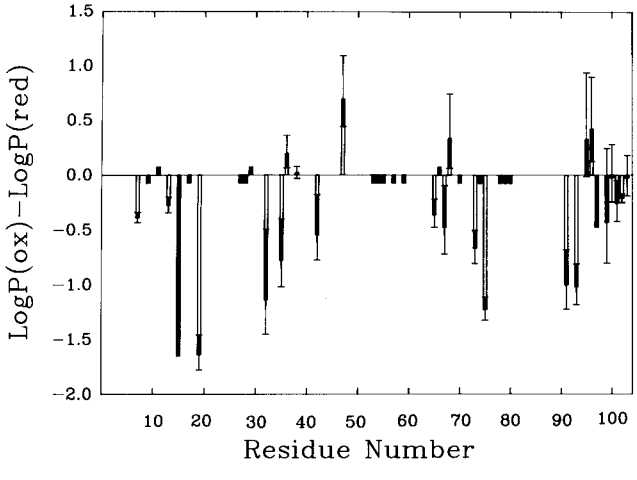

Fig. 4. Histogram of residue number versus the difference in the logarithm of the protection factor, log P, between the oxidized and reduced proteins. Error bars were calculated from the sum of the standard deviations of k_{obs} for the two oxidation states. Small solid bars represent the sign of the difference log P_{oxidized} − log P_{reduced} for residues where k_{obs} was defined in one oxidation state but not the other. Solid bars at Leu 15 and Tyr 97 represent the most positive value of the difference.

Solvent-accessible surface area, hydrogen bonding, and the minimum escape distance

Of the 30 most slowly exchanging backbone amide protons ($k_{obs} < 0.06$ h^{-1}) in either oxidation state, only Lys 73 possesses any solvent-accessible surface and 28 others, including Lys 73, are involved in hydrogen bonds. The two backbone amide nitrogens that lack both solvent-accessible surface area and hydrogen bonds are from Thr 19 and Asp 60. All but 2 of the 28 backbone amide protons are involved in backbone hydrogen bonds.

Of the 20 backbone amide protons whose value of k_{obs} is between 0.06 h^{-1} and 0.36 h^{-1} in either oxidation state, 5 possess some accessible surface and 17 are hydrogen bonded. Of the 17 hydrogen-bonded backbone amides, 10 involve backbone carbonyls, 4 involve side-chain acceptors, and 3 (from residues Phe 36, Gln 42, and Ser 47) involve buried water molecules exclusively.

Of the remaining backbone amide protons, which we assume possess k_{obs} values greater than 0.36 h^{-1}, 29 possess accessible surface and 19 are hydrogen bonded. Furthermore, 11 of the 19 hydrogen bonds involve side-chain acceptors exclusively. The shortest distance from each solvent-inaccessible backbone amide nitrogen to a solvent-accessible atom was also calculated. A plot of this distance versus k_{obs} is shown in Figure 5.

Discussion

Accessible surface area, hydrogen bonding, and distance between buried backbone amide protons and the protein surface

Generally speaking, k_{obs} is expected to be related to hydrogen bonding in the local unfolding model and to bu-

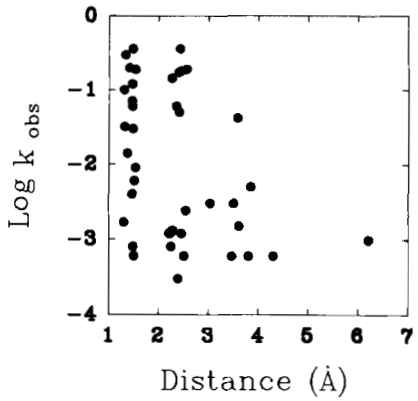

Fig. 5. Plot of distance between completely buried backbone amide nitrogens and the nearest atom with solvent-accessible surface area versus log k_{obs} for the reduced protein.

rial of labile sites in the solvent penetration model. We find that nearly all of the most slowly exchanging backbone amide protons are both buried and hydrogen bonded. Additionally, many backbone amide protons that exchange quickly possess accessible surface, lack hydrogen bonds, or both. In general, k_{obs} for backbone amide protons increases in the order: backbone hydrogen bonds < side-chain hydrogen bonds < hydrogen bonds to buried water molecules < no hydrogen bonds. Because both burial and hydrogen bonding are correlated with k_{obs}, we cannot use these general observations to distinguish between models.

A more specific difference between the models is that a dependence of k_{obs} on the distance between the buried labile proton and the nearest solvent-accessible atom might be expected for solvent penetration, but this need not be the case for local unfolding. There is no correlation between distance and k_{obs} (Fig. 5). For some of the amide nitrogens, the atom corresponding to the shortest distance possesses less than 1 Å^2 of accessible surface area and thus may not be representative. To overcome this potential problem, the average of the 10 shortest distances was also calculated, but no correlation was observed (data not shown). Such a lack of correlation has also been reported for lysozyme (Radford et al., 1992; Pedersen et al., 1993). From these observations we conclude that most of the backbone amide protons studied here exchange via local unfolding.

Secondary structure

As shown in Figures 2 and 3, regions with large P values correspond to the helices between residues 2–14, 49–56, 60–70, 70–75, and 87–103 (Louie & Brayer, 1990; Gao et al., 1990; see Kinemage 1). This is expected because residues involved in regular secondary structural elements open less frequently than residues in other regions (Englander & Kallenbach, 1984). The data also allow us to probe some subtleties of local unfolding. Backbone amide protons that form intrahelix hydrogen bonds possess large P values. There is also a decrease in P values at the ends of the C-terminal helix. The bell-shaped distribution is attributable to fraying at the ends, as predicted by Zimm and Bragg (1959) and Lifson and Roig (1961). In terms of the cooperativity of helix unfolding, the fact that there is less protection at the termini suggests that the central portion, not the entire helix, unfolds cooperatively. In the other helices, superimposed upon the bell shape is a trend toward a decrease in P values at the N-terminus and an increase at the C-terminus. This can be interpreted as an interaction of the hydroxyl ion catalyst with the helix dipole and is expected to be more pronounced for solvent penetration than for local unfolding.

Comparing the log P values from Figure 2 to those for oxidized horse cytochrome c calculated from data given by Wand et al. (1986), Paterson et al. (1990), and Mayne et al. (1992) indicates that the horse protein tends to exhibit larger P values than the C102T variant. This is in agreement with the observation that the horse protein exhibits a larger ΔG_d at 300 K (Betz & Pielak, 1992). Comparing the log P values from Figure 3 to values calculated for the N-terminal helix of horse cytochrome c (Wand et al., 1986) shows similarities between the two proteins. Both exhibit a small amount of protection until approximately Phe 10, where protection increases in both proteins (Wand et al., 1986).

The character of P values within type II β-turns supports the local unfolding model. Turns tend to be located at the surface of proteins (Rose et al., 1985). Type II β-turns in cytochromes c occur at residues 21–24, 32–35, 35–38, 43–46, and 75–78. The amide protons of the conserved glycine residues at the third position of these turns possess small P values. The amide protons of such conserved glycines can only participate in nonlocal hydrogen bonds. On the other hand, the backbone amide proton of the last residue in each turn, which is involved in a hydrogen bond to the carbonyl oxygen of the first residue, tends to exhibit larger P values. Therefore, even though turns are close to the surface, hydrogen bonding, not solvent exposure, controls the P values.

Although Ω-loops do not possess repeating motifs, they are an important and abundant form of secondary structure (Fetrow & Rose, 1989). Eukaryotic cytochromes c possess four such loops: loop A between residues 18 and 32, loop B between 34 and 43, loop C between 40 and 54, and loop D between 70 and 84 (Fetrow et al., 1989). In loop A, five backbone amide protons exhibit log P values greater than 1.5 (Figs. 2, 3). Additionally, the π proton of the imidazole ring of His 18, whose τ nitrogen is axially coordinated to the heme iron, exchanges slowly in the reduced protein. Two of the five backbone amide protons, Thr 19 and Val 28, are rare examples of amide protons that seem to lack hydrogen bonds yet exhibit substantial protection. In loops B and C, the backbone amide protons of Phe 36, Asn 42, and Ser 47 all show sub-

stantial protection, yet appear to be hydrogen bonded to only buried water molecules. Loop D also possesses many highly protected sites. These data show that despite the lack of regular structure, Ω-loops are stable structural units.

Supersecondary structure

The data for the helices show their relative stability and suggest a path for unfolding of iso-1-cytochrome *c*. The N-terminal helix, which is closest to the outside of the protein, covers the C-terminal helix, which, in turn, covers the 60s helix (Kinemage 1). Inspection of Figures 2 and 3 shows that the C-terminal helix and the 60s helix are more protected than the N-terminal helix. This observation is consistent with the idea that the N-terminal helix unfolds before the other two helices. The relative P values for the terminal helices is in agreement with experiments performed on C- and N-terminal peptides of horse cytochrome *c*, which suggest that the isolated C-terminal helix possesses more secondary structure (Kuroda, 1993). Genetic studies of yeast iso-1-cytochrome *c* also support the idea of more stable structure in the C-terminal helix. That is, the N-terminal helix is less tolerant of substitutions than is the C-terminal helix (Auld & Pielak, 1991; Fredericks & Pielak, 1993).

Unlike the C102T variant, the horse protein exhibits larger P values for the N-terminal helix and smaller P values for the C-terminal helix. It is not clear why the N-terminal helix of horse cytochrome *c* exhibits larger P values than the C-terminal helix. Larger values of P in the C-terminal helix compared to the N-terminal helix are observed for iso-1-cytochrome *c*, *Rhodobacter capsulatus* cytochrome c_2 (Gooley et al., 1991), and *Pseudomonas aeruginosa* cytochrome *c*-551 (Timkovich et al., 1992). This difference is not due to the N-terminal extension because neither cytochrome c_2 nor cytochrome *c*-511 possesses an extension. We conclude that interactions of the N-terminal helix with the C-terminal helix contribute more to the stability of horse cytochrome *c* than iso-1-cytochrome *c*.

ΔG_{op} versus ΔG_d for the oxidized protein

Inspection of Figure 2 reveals that for at least seven backbone amide protons, ΔG_{op} is greater than ΔG_d. There are several possible explanations for this behavior. Perhaps the value of k_2 approaches that of k_3 for these slowly exchanging protons, shifting exchange toward the EX_1 limit. Such an explanation has been suggested by Pedersen et al. (1993) for the most slowly exchanging backbone amide protons in lysozyme. There is no correlation between k_{obs} and the distance to the nearest solvent-exposed atom (Fig. 5). Therefore, even for these slowly exchanging protons there is no evidence for solvent penetration, but the expectation that there should be a correlation is probably an oversimplification. Perhaps the model is too simplistic and exchange cannot be described by Equation 1. If exchange occurs at the EX_2 limit, the values of k_3 may not be correct for these residues. That is, perhaps these sites are never exposed completely to solvent and therefore cannot be represented by flexible peptides—this is the gray area between the local unfolding model and the solvent-penetration model. These possibilities do not change qualitative interpretations of P values but would invalidate interpretations of ΔG_{op} for these sites.

Another possibility is that conformations higher in free energy than the denatured state are being detected. These conformations cannot represent the activated complex and, in fact, they need not be on the folding path. If they are on the path, they represent crenellations on the free energy surface above the level of the denatured state between the activated complex and the native state. These explanations have a common aspect—regions of the protein with very slowly exchanging backbone amide protons possess stable structure even in high-energy conformations. It is interesting to note that the side chains of His 18, Leu 32, Leu 68, and Arg 91 (Fig. 2) are highly conserved, possess small crystallographic temperature factors, and pack against the heme (Louie et al., 1988; Louie & Brayer, 1990), suggesting that these residues form a stable "core" that surrounds the heme in these high-energy states. Backbone amide protons close in sequence to these slowly exchanging sites can exchange much more quickly, supporting the idea of a nonpolar core. The observation of vastly difference rates for residues close in the primary structure is suggestive of solvent penetration.

The increase in ΔG_{op} upon reduction

As shown in Figure 4, the difference $\log P_{\text{oxidized}} - \log P_{\text{reduced}}$ is negative for most residues. The observation that ΔG_{op} increases upon reduction shows that the reduced form is more stable and is supported by many other studies (reviewed by Moore & Pettigrew [1990], Bixler et al. [1992], and Hilgen-Willis et al. [1993]). The largest differences for iso-1-cytochrome *c* represent an increase in stability upon reduction of approx. 2 kcal mol^{-1}, similar to the value reported for *Rhodobacter capsulatus* cytochrome c_2 (Gooley et al., 1991). Furthermore, k_{obs} for the π proton of His 18 and the indole proton of Trp 59 can be determined in the reduced C102T variant, but these resonances are absent after less than an hour in the oxidized protein. The dependence of k_{obs} on oxidation state is also observed for other cytochromes *c* (Patel & Canuel, 1976; Moore et al., 1980; Yu & Smith, 1988, 1990).

Considering the other residues for which data are available, and the fact that P values for the reduced and oxidized proteins show similar patterns, it is clear that the increased stability is not restricted to one area of the protein. The increase in ΔG_{op} upon reduction is not due to

large differences in average native structures of the two oxidation states because the structures of reduced and oxidized iso-1-cytochrome *c* are very similar (Gao et al., 1991; Berghuis & Brayer, 1992), as is true for other cytochromes *c* (Takano & Dickerson, 1981; Williams et al., 1985; Feng et al., 1990).

ΔG_{op} versus ΔG_d for the reduced protein

Using a combination of chemical denaturation data for the oxidized protein, electrochemical data for chemically (urea or guanidinium chloride) denatured states, and a Born–Haber cycle, ΔG_d for the reduced protein at 300 K, pH 4.6, is between 14.9 and 16.6 kcal mol^{-1} (Bixler et al., 1992; Hilgen-Willis et al., 1993). This corresponds to a log *P* between 11 and 12. Taken together with the data in Figure 3, this means that for the reduced protein ΔG_{op} is much smaller than ΔG_d. In fact, the largest values of ΔG_{op} in the reduced protein are about half the smallest value of ΔG_d. Thus, the denatured state of the reduced protein is much higher in free energy than the highest energy native forms that we can detect. By analogy to the discussion for the oxidized protein, even higher energy native states are significantly populated for the reduced protein, but in these states all labile protons have exchanged, making them invisible to NMR. Another possibility concerns the axial ligands to the heme iron, which are supplied by side-chain atoms of His 18 and Met 80. Upon reaching a conformation where an axial ligand bond is broken, the protein oxidizes. This also makes any higher energy conformation for the reduced protein invisible.

Why is ΔG_d much larger than ΔG_{op} for the reduced protein, whereas the opposite is true for certain residues of the oxidized protein? We suggest that the accessibility of locally unfolded conformations for the two oxidation states is different and propose that the difference involves the ligation state of the heme iron in high-energy conformations. The native oxidized protein can access conformations where one or both axial ligand bonds to the iron are broken (Muthukrishnan & Nall, 1991), but for the reduced protein these conformations are less accessible.

Conclusions

The behavior of the majority of backbone amide protons is consistent with the local unfolding model in the EX_2 limit. Only for protons that may not fit the EX_2 limit and appear to form a nonpolar core surrounding the heme do we find evidence consistent with solvent penetration.

Three different types of secondary structure were investigated. First, the cooperative unit for the unfolding of helices involves only their central portion. Second, β-turns, although located on the outside of the protein, exhibit quite stable hydrogen bonds between their first and last residues. Third, despite having no regular hydrogen-bonding pattern, Ω-loops are stable units of secondary structure.

Exchange is slower in the reduced form of the protein, consistent with this form being more stable. The native state of iso-1-cytochrome *c* includes conformations in which the axial ligand bonds to the heme iron are disrupted, although these conformations are of higher free energy in the reduced protein. The oxidized protein has more conformations accessible in the native state than the reduced protein, and it appears that some of these conformations have a higher free energy than in the denatured state.

Materials and methods

Sample preparation

The production of the C102T variant was described by Cutler et al. (1987). The protein was purified using a fast-performance liquid chromatography-modified version of an older method (Sherman et al., 1968). To prepare the oxidized sample, 40 mg of the C102T variant were oxidized as described by Betz and Pielak (1992). For samples prepared in D_2O, the stated values of pH are direct pH meter readings, uncorrected for the isotope effect (Glasoe & Long, 1960). After oxidation, the protein was concentrated to a volume of 1 mL using a Centriprep-10 (Amicon) at 4 °C. High-performance liquid chromatography-grade H_2O adjusted with HCl to pH 4.6 was used to dilute the sample. After the sample was diluted and concentrated three times, the volume was adjusted to 2.0 mL, placed in a 15-mL Corex centrifuge tube, frozen in a dry ice/ethanol bath, and lyophilized. The dried sample was resuspended in 0.750 mL of 50 mM sodium acetate D_3 (Sigma) in D_2O, pH 4.6, and transferred to an Eppendorf tube. The sample was then centrifuged to remove any precipitate, and the supernatant was placed in a 5-mm NMR tube (Wilmad 535P). Approximately 5 μL was removed and used to determine the concentration and the percentage oxidized protein using an extinction coefficient of 109.4 mM^{-1} cm^{-1} for the oxidized form at 410 nm and 130.4 mM^{-1} cm^{-1} for reduced form at 416 nm (Hilgen-Willis, 1993). The sample was greater than 95% oxidized, and the final concentration was 3 mM. The reduced protein was prepared in a similar manner except that the buffered D_2O contained 0.02 M freshly prepared ascorbate. The sample was more than 95% reduced.

NMR spectroscopy

The correlated spectroscopy (COSY) spectra were recorded at 298 K on a Bruker AMX500 spectrometer. For the oxidized protein, two-channel quadrature detection was used in t_2, and time-proportional phase incrementation (TPPI; Marion & Wüthrich, 1983) was used in t_1. For the reduced protein, TPPI was used in both dimensions. Data sets consisted of 400 t_1 increments of 40 tran-

sients and 2K data points in t_2 with a spectral width of ±4,032 Hz in both dimensions. Spectra were obtained at 0.00, 6.55, 13.1, 19.7, 26.2, 39.3, 45.8, 52.3, and 165 h for the oxidized protein and at 0.00, 6.55, 13.1, 19.7, 50.2, 56.8, 101.3, 245, 437, and 653 h for the reduced protein. The acquisition time for each spectrum was 6.6 h. The first four spectra were acquired consecutively. From examining the spectra of the reduced protein at 437 and 653 h, it appeared that the reducing agent was exhausted and some of the protein reverted to the oxidized form. Thus, only data from spectra collected within 250 h of the start of the exchange experiment were used to determine k_{obs}. Exchange experiments were collected separately on a 1 mM oxidized C102T sample using one-dimensional techniques in an attempt to obtain data for the His 18 π imidazole proton (12.85 ppm) because its crosspeak with the C5 proton (24.9 ppm) is not observed in the COSY spectra. This resonance disappears completely in less than 1 h.

Data were processed on a Silicon Graphics Personal Iris using Felix 2.0 (Hare Software, Woodinville, Washington). Resolution enhancement was performed by a combination of trapezoidal and sinebell functions in t_1 and t_2. The final digital resolution was 4.0 Hz point^{-1}. To allow the determination of crosspeak volumes, an absolute magnitude calculation was performed after transformation in t_1. Peak volumes (Vol) were normalized using Equation 2:

$$\text{Vol} = \frac{(v_c - v_0)}{(v_s - v_0)}, \qquad (2)$$

where v_c is the observed volume, v_0 is the average of 10 volumes taken at each time point for each protein in regions of the spectrum where no peaks are visible, and v_s is the volume of an internal standard for nonexchangeable crosspeaks. For the oxidized protein, the internal standard is the Thr 19 beta-gamma crosspeak. For the reduced protein, it is the average of the methine-methyl crosspeaks of the heme (Wand et al., 1986). Resonance assignments were from Gao et al. (1990, 1991).

Calculation of solvent-accessible surface area

Solvent-accessible surface areas for the heavy atoms of reduced iso-1-cytochrome *c* were calculated from the crystallographic coordinates (Louie & Brayer, 1990) using the program GEPOL92 (Silla et al., 1991), van der Waals radii given by Lee and Richards (1971), and a probe radius of 1.4 Å. Calculations using coordinates for the oxidized protein (Berghuis & Brayer, 1992) yielded essentially identical results. For the purpose of comparing k_{obs} to solvent-accessible surface area, we assigned a value of 0.36 h^{-1} to k_{obs} for backbone amide protons whose crosspeaks disappear after the first time point.

Supplementary materials on Diskette Appendix

A table containing the values of k_{obs}, k_3, and log P for the reduced and oxidized forms of the C102T variant of *Saccharomyces cerevisiae* iso-1-cytochrome *c* at 298 K, pH 4.6, is included on the Diskette Appendix.

Acknowledgments

This work was supported by an NIH FIRST award (GM42501). J.L.M. was supported partially by an NIH training grant (GM08332). D.S.A. and D.F.D. were supported partially by U.S. Department of Education Fellowships, and S.F.B. was supported partially by the Program in Molecular Biology and Biotechnology at the University of North Carolina. We thank Terry Oas for helpful discussions and S. Walter Englander and Leland Mayne for providing preprints describing the new parameters for calculating k_3.

References

Auld, D.S. & Pielak, G.J. (1991). Constraints on amino acid substitutions in the N-terminal helix of cytochrome *c* explored by random mutagenesis. *Biochemistry 30*, 8684–8690.

Bai, Y., Milne, J.S., Mayne, L., & Englander, S.W. (1993). Primary structure effects on peptide group hydrogen exchange. *Proteins Struct. Funct. Genet. 17*, 75–86.

Berghuis, A.M. & Brayer, G.D. (1992). Oxidation state-dependent conformational changes in cytochrome *c*. *J. Mol. Biol. 223*, 959–976.

Betz, S.F. & Pielak, G.J. (1992). Introduction of a disulfide bond into cytochrome *c* stabilizes a compact denatured state. *Biochemistry 31*, 12337–12344.

Bixler, J., Bakker, G., & McLendon, G. (1992). Electrochemical probes of protein folding. *J. Am. Chem. Soc. 114*, 6938–6939.

Connelly, G.P., Bai, Y., Jeng, M.-F., & Englander, S.W. (1993). Isotope effects in peptide group hydrogen exchange. *Proteins Struct. Funct. Genet. 17*, 87–92.

Cutler, R.L., Pielak, G.J., Mauk, A.G., & Smith, M. (1987). Replacement of cysteine-107 of *Saccharomyces cerevisiae* iso-1-cytochrome *c* with threonine: Improved stability of the mutant protein. *Protein Eng. 1*, 95–99.

Ellis, L.M., Bloomfield, V.A., & Woodward, C.K. (1975). Hydrogen-tritium exchange kinetics of soybean trypsin inhibitor (Kunitz). Solvent accessibility on the folded conformation. *Biochemistry 14*, 3413–3419.

Englander, J.J., Calhoun, D.B., & Englander, S.W. (1979). Measurement and calibration of peptide group hydrogen-deuterium exchange by ultraviolet spectrophotometry. *Anal. Biochem. 92*, 517–524.

Englander, S.W. & Kallenbach, N.R. (1984). Hydrogen exchange and structural dynamics of proteins and nucleic acids. *Q. Rev. Biophys. 16*, 521–655.

Feng, Y., Roder, H., & Englander, S.W. (1990). Redox-dependent structure change and hyperfine nuclear magnetic resonance shifts in cytochrome *c*. *Biochemistry 29*, 3494–3504.

Fetrow, J.S., Cardillo, T.S., & Sherman, F. (1989). Deletion and replacements of omega loops in yeast iso-1-cytochrome *c*. *Proteins Struct. Funct. Genet. 6*, 372–381.

Fetrow, J.S. & Rose, G.D. (1989). Loops in globular proteins: A novel category of secondary structure. In *Protein Folding* (Gierasch, L.M. & King, J., Eds.), pp. 18–28. American Association for the Advancement of Science, Washington, D.C.

Fredericks, Z.L. & Pielak, G.J. (1993). Exploring the interface between the N- and C-terminal helices of cytochrome *c* by random mutagenesis within the C-terminal helix. *Biochemistry 32*, 929–936.

Gao, Y., Boyd, J., Pielak, G.J., & Williams, R.J.P. (1991). Comparison of reduced and oxidized yeast iso-1-cytochrome *c* using paramagnetic shifts. *Biochemistry 30*, 1928–1934.

Gao, Y., Boyd, J., Williams, R.J.P., & Pielak, G.J. (1990). Assignment of proton resonances, identification of secondary structural elements, and analysis of backbone chemical shifts for the C102T variant of yeast iso-1-cytochrome *c* and horse cytochrome *c*. *Biochemistry 29*, 6994–7003.

Glasoe, P.K. & Long, F.A. (1960). Use of glass electrodes to measure acidities in deuterium oxide. *J. Phys. Chem. 64*, 188–190.

Gooley, P.R., Zhao, D., & MacKenzie, N.E. (1991). Comparison of amide proton exchange in reduced and oxidized *Rhodobacter capsulatus* cytochrome c_2: A ^1H-^{15}N NMR study. *J. Biomol. NMR 1*, 145–154.

Gregory, R.B., Crabo, L., Percy, A.J., & Rosenberg, A. (1983). Water catalysis of peptide hydrogen isotope exchange. *Biochemistry 22*, 910–917.

Hilgen-Willis, S. (1993). Spectroscopic, electrochemical, thermodynamic, and genetic studies of *Saccharomyces cerevisiae* iso-1-cytochrome *c* with substitutions at positions 6, 10, 20, 52, 82, 97, and 102. Doctoral Dissertation, University of North Carolina, Chapel Hill.

Hilgen-Willis, S., Bowden, E.F., & Pielak, G.J. (1993). Dramatic stabilization of ferricytochrome *c* upon reduction. *J. Inorg. Biochem. 51*, 649–653.

Hvidt, A. & Nielsen, S.O. (1966). Hydrogen exchange in proteins. *Adv. Protein Chem. 21*, 287–386.

Kuroda, Y. (1993). Residual helical structure in the C-terminal fragment of cytochrome *c*. *Biochemistry 32*, 1219–1224.

Lee, B. & Richards, F.M. (1971). The interpretation of protein structures: Estimation of static accessibility. *J. Mol. Biol. 55*, 379–400.

Lifson, S. & Roig, A. (1961). On the theory of the helix–coil transition in polypeptides. *J. Chem. Phys. 34*, 1963–1974.

Linderstrøm-Lang, K.U. (1958). Deuterium exchange and protein structure. In *Symposium on Protein Structure* (Neuberger, A., Ed.), pp. 23–34. Methuen, London.

Louie, G.V. & Brayer, G.D. (1990). High-resolution refinement of yeast iso-1-cytochrome *c* and comparisons with other eukaryotic cytochromes *c*. *J. Mol. Biol. 214*, 527–555.

Louie, G.V., Hutcheon, W.L.B., & Brayer, G.D. (1988). Yeast iso-1-cytochrome *c*. A 2.8 Å resolution three-dimensional structure determination. *J. Mol. Biol. 199*, 295–314.

Marion, D. & Wüthrich, K. (1983). Application of phase sensitive two-dimensional correlated spectroscopy (COSY) for measurements of ^1H-^1H spin–spin coupling constants in proteins. *Biochem. Biophys. Res. Commun. 113*, 967–974.

Mayne, L., Paterson, Y., Cerasoli, D., & Englander, S.W. (1992). Effect of antibody binding on protein motions studied by hydrogen-exchange labeling and two-dimensional NMR. *Biochemistry 31*, 10678–10685.

McDonald, C.C. & Phillips, W.D. (1973). Proton magnetic resonance studies of horse cytochrome *c*. *Biochemistry 12*, 3170–3186.

Molday, R.S., Englander, S.W., & Kallen, R.G. (1972). Primary structure effects on peptide group hydrogen exchange. *Biochemistry 11*, 150–158.

Moore, G.R., de Aguiar, A.B.V.P., Pluck, N.D., & Williams, R.J.P. (1980). The properties and functions of tryptophan in proteins. In *Biochemical and Medical Aspects of Tryptophan Metabolism* (Hayaishi, O., Ishimura, Y., & Kido, R., Eds.), pp. 83–94. Elsevier/North-Holland, Amsterdam.

Moore, G.R. & Pettigrew, G.W. (1990). *Cytochromes c. Evolutionary, Structural and Physicochemical Aspects*. Springer-Verlag, Berlin.

Muthukrishnan, K. & Nall, B.T. (1991). Effective concentrations of amino acid side chains in an unfolded protein. *Biochemistry 30*, 4706–4710.

Patel, D.J. & Canuel, L.L. (1976). Nuclear magnetic resonance studies of slowly exchanging peptide protons in cytochrome *c* in aqueous solution. *Proc. Natl. Acad. Sci. USA 73*, 1398–1402.

Paterson, Y., Englander, S.W., & Roder, H. (1990). An antibody binding site on cytochrome *c* defined by hydrogen exchange and two-dimensional NMR. *Science 249*, 755–759.

Pedersen, T.G., Thomsen, N.L., Andersen, K.V., Madsen, J.C., & Poulsen, F.M. (1993). Determination of the rate constants k_1 and k_2 of the Linderstrøm-Lang model for protein amide hydrogen exchange: A study of the individual amides in hen egg-white lysozyme. *J. Mol. Biol. 230*, 651–660.

Perrin, C.L. (1989). Proton exchange in amides: Surprises from simple systems. *Acc. Chem. Res. 22*, 268–275.

Radford, S.E., Buck, M., Topping, K.D., Dobson, C.M., & Evans, P.A. (1992). Hydrogen exchange in native and denatured states of hen egg-white lysozyme. *Proteins Struct. Funct. Genet. 14*, 237–248.

Roder, H., Wagner, G., & Wüthrich, K. (1985). Amide proton exchange in proteins by EX_1 kinetics: Studies of the basic pancreatic trypsin inhibitor at variable p^2H and temperature. *Biochemistry 24*, 7396–7407.

Rose, G.D., Gierasch, L.M., & Smith, J.A. (1985). Turns in peptides and proteins. *Adv. Protein Chem. 37*, 1–109.

Sherman, F., Stewart, J.W., Parker, J.H., Inhaber, E., Shipman, N.A., Putterman, G.J., Gardisky, R.L., & Margoliash, E. (1968). The mutational alteration of the primary structure of yeast iso-1-cytochrome *c*. *J. Biol. Chem. 243*, 5446–5456.

Silla, E., Tuñón, I., & Pascual-Ahuir, J.L. (1991). GEPOL: An improved description of molecular surfaces II. Computing the molecular area and volume. *J. Comput. Chem. 12*, 1077–1088.

Takano, T. & Dickerson, R.E. (1981). Conformational change in cytochrome *c*. II. Ferricytochrome *c* refinement at 1.8 Å and comparison with the ferrocytochrome *c* structure. *J. Mol. Biol. 153*, 95–115.

Timkovich, R., Walker, L.A., II, & Cai, M. (1992). Hydrogen exchange in *Pseudomonas* cytochrome *c*-551. *Biochim. Biophys. Acta 1121*, 8–15.

Wand, A.J., Roder, H., & Englander, S.W. (1986). Two-dimensional ^1H NMR studies of cytochrome *c*: Hydrogen exchange in the N-terminal helix. *Biochemistry 25*, 1107–1114.

Williams, G., Clayden, N.J., Moore, G.R., & Williams, R.J.P. (1985). Comparison of the solution and crystal structures of mitochondrial cytochrome *c*: Analysis of the paramagnetic shifts in the nuclear magnetic resonance spectrum of ferricytochrome *c*. *J. Mol. Biol. 183*, 447–460.

Woodward, C.K. & Hilton, B.D. (1979). Hydrogen exchange kinetics and internal motions in proteins and nucleic acids. *Annu. Rev. Biophys. Bioeng. 8*, 99–127.

Yu, L.P. & Smith, G.M. (1988). ^{15}N and ^1H NMR studies of *Rhodospirillum rubrum* cytochrome c_2. *Biochemistry 27*, 1949–1956.

Yu, L.P. & Smith, G.M. (1990). Characterization of pH-dependent conformational heterogeneity in *Rhodospirillum rubrum* cytochrome c_2 using ^{15}N and ^1H NMR. *Biochemistry 29*, 2920–2925.

Zhang, Z. & Smith, D.L. (1993). Determination of amide hydrogen exchange by mass spectrometry: A new tool for protein structure elucidation. *Protein Sci. 2*, 522–531.

Zimm, B.H. & Bragg, J.K. (1959). Theory of the phase transition between helix and random coil in polypeptide chains. *J. Chem. Phys. 31*, 526–535.